GEOLOGICAL INVESTIGATIONS

015088

Anvil District

1971 Exploration Program

D. S. Jennings

Abstract:

Three main lithologic units comprise the Eocambrian section of the Anvil district on the southwestern flank of the Anvil Arch (Figure I). In ascending stratigraphic order they are: a) Biotite-muscovite schist b) Calc-silicate gneiss and c) Biotite-muscovite phyllite. All units have highly variable thicknesses and are grossly conformable to the main penetrative metamorphic foliation, S_2. Massive stratabound lead-zinc sulfide deposits occur in both the schist and phyllite units. The Faro orebodies were deposited in the the protolith of the schist unit while the Vangorda, Swim, Firth and Champ sulfide bodies were deposited in the phyllite protolith.

Five periods of deformation and metamorphism, in addition to the intrusion of the Anvil Batholith, can be systematically mapped in much of the district. The interrelationship of this complex deformational history and the seemingly simple regional stratigraphy are reviewed. Grades of regional metamorphism encountered thus far are dominantly lower to middle amphibolite facies. Rocks near Blind Creek may be transitional to the upper green-schist facies.

Bulk compositional data suggest the Eocambrian section in the Anvil district represents a quiet water accumulation of variably calcareous pelitic sediments. Presence of graphite in many parts of the section implies reducing conditions during deposition. A deep, marine basin of mio-geosynclinal character is the most probable depositional environment.

Current information suggests a syngenetic origin for the sulfide deposits in the Anvil district. No genetic relationship between sulfide mineralization and the Anvil batholith is apparent. Original bedding, S_0, in graphitic, quartz-rich horizons in the schist and phyllite units appears to be the primary, structural control of sulfide deposition, emphasizing the need for a thorough understanding of the deformational history of the belt.

The spatial association of sulfides, quartzite, graphitic schist and muscovite-biotite schist and their position relative to the lower calc-silicate gneiss contact should be noted. It is emphasized that all stratigraphic unit contacts are conformable to the main metamorphic foliation (S_2) in the pit. This foliation is used as the plane of reference for measuring stratigraphic thicknesses relative to an arbitrarily chosen "top direction" on the southwestern flank of the Anvil Arch. Consequently, the stratigraphic section given in Table I bears no necessary relation to original stratigraphic thicknesses or top directions. It is constructed merely as a working stratigraphic section to assess the current spatial distribution of rock units in the Faro area. Consideration of rock origins will be deferred to a separate section later in this report.

Four rock units intrude metamorphic rocks exposed in the pit. Small, fine grained, dark green, chloritic, metamorphosed andesite dikes are the oldest of the four intrusions since they are the only intrusive units cut by the main metamorphic foliation. These dikes show irregular intrusive contacts, and are volumetrically least important of the four intrusive units. Age relationships of the three remaining units cannot be discerned in the pit.

The hornblende-biotite quartz diorite at the north end of the pit is, volumetrically, the largest intrusive unit exposed. It is a coarse grained, light gray-green diorite with conspicuous phenocrysts of hornblende, biotite and quartz. Joint and fault sets pervade the diorite giving it a prominent blocky surface exposure. Weathering occurs to considerable depths (+ 200 feet) along these fracture sets. The exact nature of the weathering products is unknown at present. Little can be discerned of the diorite's general geometry and genetic relation (if any) to the Anvil Batholith from present exposures in the pit.

The fine grained, gray, biotite diorite dike exposed near the southern margin of the pit is probably related to the main diorite mass just discussed. Although black, pseudo-hexagonal prisms of biotite form the main phenocrepts, small amounts of hornblende are also present suggesting a genetic connection.

TABLE I: Stratigraphic Section Through the Anvil Pit

Top	Unit	Description	Thickness
	Calc-silicate gneiss (2a, b)	Finely banded to lenticularly laminated gneiss made up of alternating, fine grained, light green diopside-quartz-feldspar-calcite bands and dark brown to purplish brown, finely crystalline biotite-muscovite phyllite layers. Unit contains occasional, thin, lenticular, moderately coarse-grained, white marble laminae and is calcareous throughout. Base of unit characterized by disappearance of diopside-rich bands and development of thin chlorite schist and amphibolite units.	>400 feet
	Biotite-muscovite schist with graphitic schist interbands (1a, 1b)	Dark brown, homogeneous, finely crystalline, biotite-rich, laminarly foliated schist with black graphitic schist interbands conformable to S_2 in the central portion of the unit. Graphitic schist grades laterally into the biotite-muscovite schist along strike. A staurolite rich zone occurs in the upper portion of the unit beneath the calc-silicate gneiss.	100 feet
	Muscovite-biotite schist (1c)	Silvery gray, coarsely crystalline, strongly schistose, porphyroblastic muscovite - biotite chlorite schist. Shows broad, gradational contact with overlying biotite-muscovite schist and sharp contact with underlying quartzite.	150 feet
	Quartzite	Gray, medium grained, discontinuous, muscovite-pyrite rich quartzite in gradational contact with underlying massive sulfides. Foliation in the quartzite is defined by a preferred orientation of phyllosilicate minerals which parallels compositional banding in the massive sulfides. Quartzite is free of Pb/Zn sulfides	0-15 feet

Unit	Description	Thickness
Massive sulfides (1c)	Black, massive, sphalerite, galena, pyrite mass with minor chalcopyrite in quartzite. Unit of variable thickness often showing prominent pyrite banding parallel to foliation in the metamorphic host rock. Lower contact of sulfides is gradational into underlying quartzite. In general, unit consists of massive, Pb/Zn sulfides, stratabound in quartzite and stratiform with respect to the main penetrative metamorphic foliation.	150 feet (average)
Quartzite (1d)	Identical to and part of the quartzite overlying the massive sulfides. Unit shows a sharp contact with the underlying muscovite-biotite schist.	0-15 feet
Muscovite-biotite schist (1c)	Identical to and part of the preceeding muscovite-biotite schist unit. Quartzite with interbanded sulfides occurs as a horizon within this unit.	> 100 feet

Base

---------- = Gradational contact

_____ = Sharp contact

A small, fine grained, pink quartz monzonite to granodiorite dike is exposed in the northwestern corner of the pit. No physical connection of this dike and the main diorite mass is evident despite their proximity. The dike rocks are heavily altered to a punky mass of pinky-brown clay minerals and relict quartz phenocrysts. This alteration may be due to a reaction between a volatile rich granodiorite melt and the underlying sulfide mass.

Deformational History:

Five deformational events are recognized in the metamorphic rocks exposed in the pit. A summary of the features produced during each event is given in Table 2.

The earliest recognizable structural feature is the S_1 foliation which occurs as discreet microlithions between S_2 surfaces. The approximate strike of S_1 is 120°-150° dipping subvertically. S_1 is best preserved in the calc-silicate gneiss and biotite-muscovite schist units in the pit. Where visible, this foliation is defined by a preferred planar orientation of biotite and muscovite suggesting a wide range of formative metamorphic conditions (greenschist to upper amphibolite facies). Laminar to thin compositional banding also parallels S_1. The significance of this banding and its possible relation to original bedding cannot be deciphered within the confines of the pit. S_1 is best preserved in the hinges of F_2 folds (Table 2) and is transposed parallel to the younger S_2 foliation on the limbs of these folds.

The second deformation, D_2, produced the main penetrative metamorphic foliation imparting a layered appearance to rocks in the pit. Average S_2 strike is 110° - 120° dipping 20° to 60° southwest. Rock unit contacts are parallel to this foliation as described previously. S_2 cuts S_1 and folds it into recumbent, close to tight slip (passive flow, shear etc.) folds here termed F_2. In general only limited, mesoscopic examples of this fold generation are evident. S_2 is axial planar to F_2 transposing S_1 parallel to itself on the limbs of these folds. The intersection of S_1 and S_2 in the hinge region defines the L_2 lineation

TABLE 2: Deformational Events and Features Produced in Metamorphic Rocks of the Anvil Pit

Event	Structural Features Produced		
	Planar	Linear	Fold Generation
D_1	S_1; earliest penetrative metamorphic foliation, strike 120°-150°, dip subvertical	None detected	None detected
D_2	S_2; main penetrative metamorphic foliation, strike 110°-120°, dip 20°-60° SW	L_2; crenulation lineation parallel to S_1-S_2 intersection, preserved only on hinges of F_2 folds, trend 120°-150°, plunge shallow to northwest	F_2; open to tight, parallel to similar slip folds in S_1, S_2 axial planar to F_2, L_2 parallel to F_2 axes
D_3	S_3; weak, non-penetrative metamorphic foliation, strike 150°-160°, dip subvertical	L_3; strong, penetrative crenulation lineation parallel to S_2-S_3 intersection, trend 150°-160° plunge 20°-40° southeast	F_3; open to close, parallel flexural slip folds in S_2, where developed S_3 is axial planar to F_3, L_3 parallel to F_3 axes
D_4	S_4; weak, non penetrative metamorphic foliation, strike 110°-120°, dip subvertical; series of thrust faults parallel to S_2	L_4; weak, non-penetrative crenulation lineation parallel to S_2-S_4 intersection, trend 110°-120° plunge shallow northwest or south east	F_4; open to close, parallel doubly plunging flexural slip folds in S_2, where developed S_4 is axial planar to F_4, L_4 parallel to F_4 axes
D_5	S_5; very weak, non-penetrative metamorphic foliation, strike 60° - 80°, dip subvertical	L_5; very weak, non-penetrative, crenulation lineation parallel to S_2-S_5 intersection, trend 60°-80° plunge shallow northeast or south west	F_5; open to close, parallel, doubly plunging flexural slip folds in S_2, where developed, S_5 is axial planar to F_5, L_5 parallel to F_5 axes

which parallels a well developed crenulation lineation trending 120°-150° and plunging shallowly to the northwest. In all probability, this crenulation lineation developed in response to flexural slip (slip along S_1 surfaces) during the beginning of the D_2 event, L_2 is now preserved only in the hinge zones of F_2 folds, since S_1 has been transposed parallel to the developing S_2 foliation in the limbs of these folds as deformation proceeded. Thus, D_2 changed from early active behaviour of S_1 to passive behaviour in the latter stages of deformation.

Both the D_1 and D_2 events have produced penetrative planar and linear features on the scale of the pit. Metamorphism associated with the D_1 event is, at least, of biotite grade and probably higher. D_2 metamorphism is of middle amphibolite facies rank. These events represent the most important dynamothermal metamorphisms recorded in the pit rocks and, for convenience, are referred to as an early deformational package. The metamorphic fabric produced by these events is the frame of reference for measurement of fabrics related to subsequent events. Rock geometry produced by the early deformational package is summarized in Figure 3. Because of their mesoscopic scale, effects of these early deformations are not readily visible in Figure 2. The most obvious feature related to these events is the general parallelism of stratigraphic unit contacts to S_2. One moderately sized F_2 fold is exposed in quartzites on the 3990 bench, east wall. This fold is refolded about a later F_4 axis.

D_3 deformation and metamorphism produced a weak, non-penetrative, metamorphic foliation, S_3, axial planar to F_3 folds in S_2. S_3 strikes 150° - 160° and has a subvertical dip. Its intersection with S_2 is parallel to a penetrative, crenulation lineation, L_3, trending 150°-160° and plunging 20°-40° southwest. L_3 parallels the axes of F_3 folds which are open to close, parallel, flexural slip folds in S_2. The L_3 crenualtion lineation developed in response to interfolia slip along S_2 during the formation of F_3 folds at the beginning of D_3 movement. Toward the end of the D_3 event, phyllosilicates developed parallel to the axial plane of these folds defining S_3. This developing foliation began to act as the active plane of slip in F_3 folds during the last stages of deformation, but movement ceased before true slip folds developed. Movement along S_3 emphasized the amplitude of the L_3 lineation. A large family of F_3 folds constitutes an important structural feature in the northwestern end of the pit while the L_3 lineation is penetrative in the total volume of pit rocks. The amplitude of F_3 folds in the pit varies from a few inches to approximately 30 feet. Wavelengths of these folds average about 50 feet for

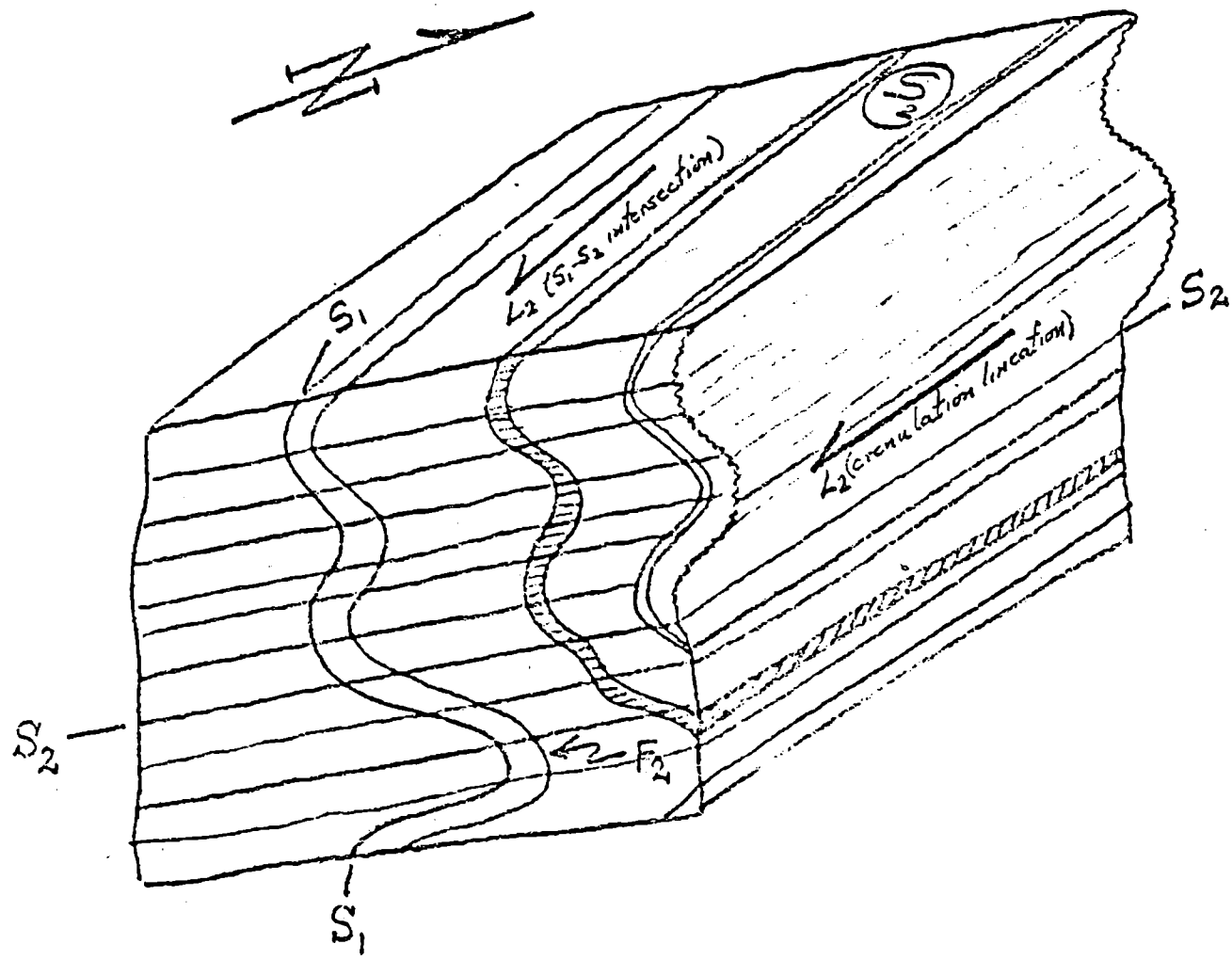

FIGURE 3: ROCK GEOMETRY PRODUCED BY THE D_1 & D_2 EVENTS

the larger folds. Grade of metamorphism associated with the D_3 event is uncertain at present since only biotite and muscovite can be recognized visually as stable minerals in the plane of S_3.

D_4 deformational features superimposed upon the D_1, D_2 and D_3 fabrics include a non-penetrative, axial planar, metamorphic foliation, S_4, striking 110°-120° dipping subvertically; a non-penetrative crenulation lineation, L_4; and the open to close, doubly plunging, parallel, flexural slip, F_4 folds in S_2 themselves. L_4 is parallel to F_4 axes; it trends 110°-120° and plunges shallowly northwest or southeast. F_4 folds are genetically similar to those of the F_3 generation and are distinguished by their unique orientation in space and by deformation of the pre-existing D_3 fabric. Folds of this generation are the largest recognized in the pit. Approximate amplitudes of the F_4 folds on the east wall (Figures 2 and 4) are 50-120 feet (increasing northward) with wavelengths of approximately 250 feet. These folds appear to decrease in amplitude rapidly with depth in the exposed portion of the orebody suggesting significantly different mechanical behaviours between the sulfides and country rocks (Figure 4). The doubly plunging character of the F_4 folds in conjunction with their size emphasize their significance to problems of ore control. A tabular sheet of massive sulfides extends upward from the crest of the northernmost anticline on the east pit wall. (Figures 2, 4) Absence of enveloping quartzite and fault contacts with muscovite-biotite schist suggest this sulfide sheet is the remobilized equivalent of the north limb of the fold transported along fault surfaces either during the last stages of D_4 movement or D_5 faulting.

In addition to the folding just described, thrust faulting occurred during D_4 along pre-existing S_2 surfaces. At least six thrusts can be recognized on the west wall of the pit (Figure 2). Slip lines for these thrusts appear to be normal to F_4 axes and D_4 boudin lines indicating a genetic relationship between thrusting and F_4 folding during brittle D_4 deformation. The active character of S_2 during this deformation is emphasized. Allochthonous movement during thrusting has been to the northeast.

D_4 metamorphism is, at least, biotite grade. Facies assignment must await petrographic investigation.

Features produced by the D_5 event occur only sporadically in the pit. S_5 is a very weak, non-penetrative, metamorphic foliation of at least biotite grade striking 60°-80° dipping subvertically. It is axial planar to F_5 folds which are geometrically similar to F_4 folds on a much smaller scale. F_5 folds are spatially associated with normal faults cutting the previously described thrust faults. A crenulation lineation, L_5, is parallel to the axis of F_5 folds. This lineation is produced by flexural slip along S_2 in a manner similar to L_3 and L_4. It is parallel to the S_2-S_5 intersection.

Perhaps the broad zone of northwest striking normal faults through the center of the pit (Figure 2) developed during the D_5 event. Since this fault set cuts the D_4 thrust faults and F_4 folds, the normal faulting is a very late D_4 or a post - D_4 feature. Intrusion of the hornblende-biotite quartz diorite body at the north end of the pit may have created a stress field conducive to normal faulting along its southern margin. Alternatively, relaxation of D_4 compressional stresses may have produced very late D_4 brittle failure along this broad fault zone.

In summary, the early deformations, D_1 and D_2, are characterized by ductile deformational features. The passive behaviour of older planar anisotropy during slip folding and the development of penetrative metamorphic foliations (S_1 and S_2) distinguish the early deformational package from later events. Active behaviour of existing anisotropy (S_2) during the D_3, D_4 and D_5 events allowed development of flexural slip folds and non-penetrative, axial planar, metamorphic foliations characteristic of this later deformational package. Age relationships in the deformational sequence given in Table 2 were defined by careful observation of cross-cutting structural features. A summary of post-D_5 rock geometry is given in Figure 5.

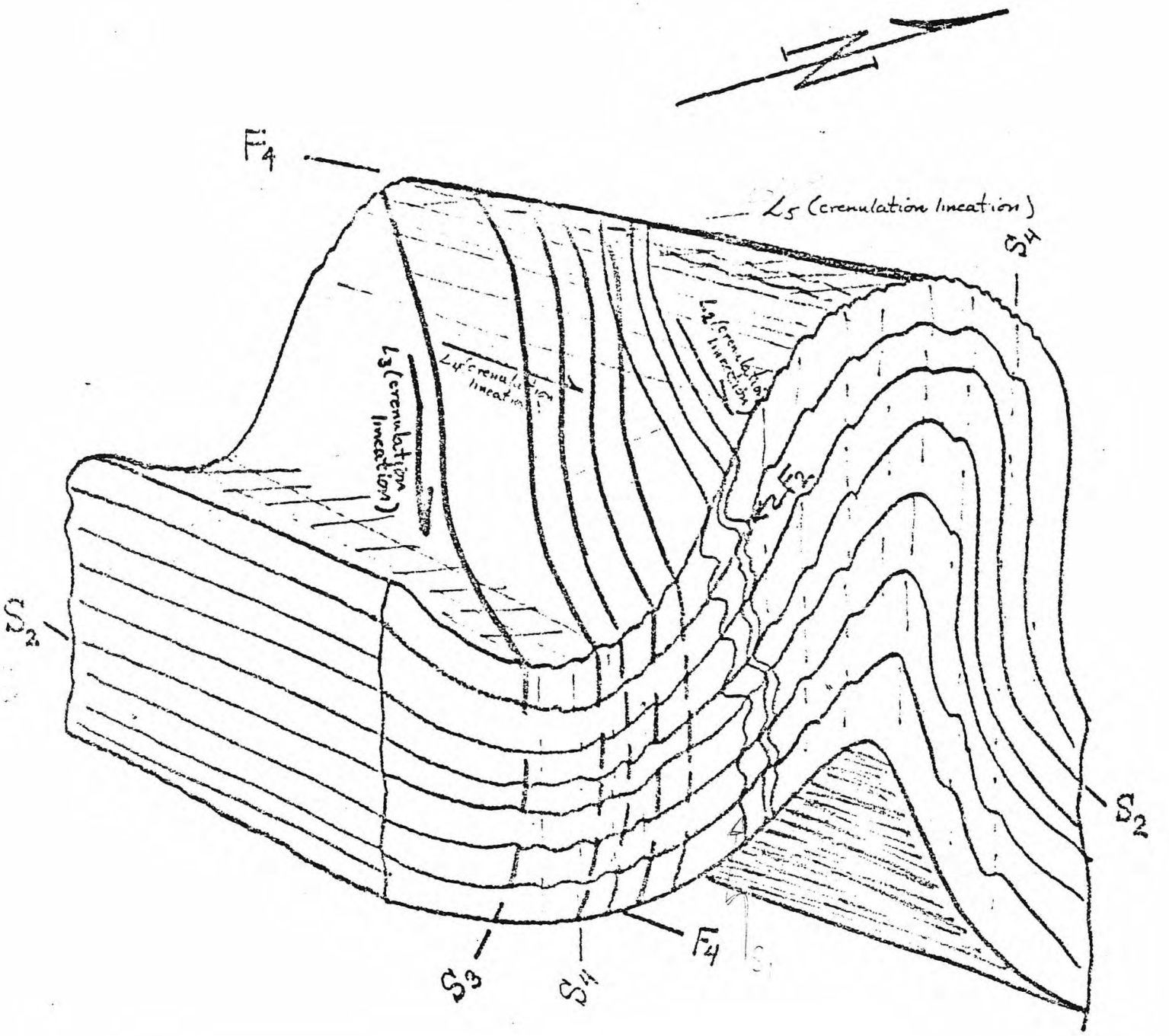

FIGURE 5: POST-D_3 ROCK GEOMETRY (F_3 & F_5 FOLDS OMITTED)

Relationship of Sulfides to Stratigraphy and Structure:

Massive sulfides in the pit occur within a quartzite unit enveloped by muscovite-biotite schists (Figure 2). The sulfide-bearing quartzite lies 200-300 feet beneath the contact of the calc-silicate gneiss and the graphitic biotite schists. The spatial association of these units must be considered in any model of sulfide genesis; their stratigraphic position within rocks of the Anvil district may be a valid exploration guide.

Five deformational events have been superimposed on the sulfide-bearing sequence. The degree to which sulfides have been transposed from their original depositional attitude into parallelism with S_1 and S_2 is unknown. Folding associated with the D_3, D_4 and D_5 events has merely crenulated the sulfide mass which is grossly conformable to S_2.

Geology of the Faro Grid:

Stratigraphy and Intrusive History:

Detailed 400 scale mapping of the area adjacent to the open pit required expansion of the stratigraphic section recognized in the pit. Above the calc-silicate gneiss unit and in gradational contact with it is a thick sequence of calcareous, gray-brown, fine grained, fissile, biotite-muscovite phyllites (unit 3a, Figure 6). Since the top of this unit is nowhere exposed on the Faro grid, estimates of its true thickness cannot be made at present. The base of the phyllite unit is defined at the uppermost extent of the light green, diopside-rich laminae in the underlying calc-silicate gneiss. Compositionally, the phyllitic partings in the calc-silicate gneiss are very similar to the main phyllite unit.

Since the detailed units underlying the calc-silicate gneiss in the pit (Table 2) cannot be recognized as systematically mappable units on the scale of the grid, they have been included in a biotite-muscovite schist unit (unit 1g, Figure 6) which is readily mappable at this scale. It is a coarsely porphyroblastic, silvery grey brown, heavily foliated schist showing variable muscovite-biotite proportions. The base of this unit is not exposed on the grid, thus no reliable estimate if its thickness can be made. The calc-silicate gneiss unit between the schist and phyllite varies in thickness between 600 and 1200 feet. An approximate stratigraphic column for the Faro grid is given in Table 3.

TABLE 3: Stratigraphic Section, Faro Grid

Top	Unit	Thickness
	Biotite-muscovite phyllite	> 2000 feet

	Calc-silicate gneiss	600-1200 feet

Base	Biotite-muscovite schist	> 2000 feet

---------- = gradational contact

As in the case of the pit, the top direction for this section is arbitrarily defined and stratigraphic unit contacts are parallel to the main metamorphic foliation. Since the biotite-muscovite schist is exposed in the core of the Anvil Arch, it is considered the oldest stratigraphic unit on the grid.

The most plausible explanation for the graphitic schists and quartzites not being mappable units in the biotite-muscovite schist is their direct spatial and presumed genetic association with sulfides. In addition, exposure along the belt underlain by the schist unit is not particularly good.

Silicated marble horizons (2b) occur within the calc-silicate gneiss. These marbles may vary from moderately coarsely crystalline, white, essentially pure, carbonate rocks to finer grained, diopside-rich, light greenish gray calc-silicate bands. They vary in thickness from 50 to 150 feet and cannot be traced over distances greater than 1000 feet because of poor exposure.

The biotite-muscovite phyllite (unit 3a) cannot be subdivided on the Faro grid. Sporadic outcrops of an apparently more muscovite-rich phyllite are encountered which may occur as a unit in the phyllite elsewhere.

Fine grained, dark green amphibolites (10a) are the oldest intrusive rocks exposed on the grid. They show intrusive contacts with the enclosing calc-silicate gneisses and are the only intrusive rock type cut by the S_2 foliation. On the basis of their outcrop pattern, these amphibolites are thought to be irregular gabbro plugs or dikes.

Rocks of the Anvil Batholith appear to be the next igneous suite to intrude the Eocambrian metamorphic section. The bulk of the batholithic rocks are coarsely crystalline biotite-quartz monzonites to biotite-granodiorites (11a) with large, characteristic, potassium feldspar megacrysts. The monzonitic and granodioritic rocks show a penetrative foliation defined by the preferred planar orientation of biotite flakes and long axes of the feldspar megacrysts. Within the plane of foliation, the long axes of these megacrysts are randomly oriented. This foliation in all likelihood is an igneous flow foliation since it bears no relation to any foliation in the country rocks. Leucocratic, unfoliated, medium crystalline, hornblende-biotite

diorites (~~14~~c) occur as border phases of the batholith at two areas along its contact on the Faro grid (Figure 6). Their genetic relationship to the monzonitic phase of the batholith is unknown at present. Contact metamorphic effects attributable to the Anvil Batholith appear to be negligible, as there is minimal development of hornfels near its contact with the country rocks. Petrographic examination of contact zone rocks will shed further light on this matter.

10E28 Coarsely porphyritic, medium to dark green, hornblende diorite dikes (~~13a~~) cut the batholithic rocks at several places on the grid. These dikes follow a northeasterly trend and may be intruded along fracture sets produced by intrusion of the batholith. The diorite mass in the north end of the pit is the largest single body in this diorite clan. A narrow (up to 100 feet) zone of contact hornfelsing is developed in the pit rocks adjacent to it. Phase assemblages in the hornfels defining its grade (s) of metamorphism have not been worked out.

Intrusion of hornblende diorite in the country rocks around zone 3 produced extensive brecciation (Figure 6). Diorite, seen as the breccia matrix, appears to have exploded its superencumbent cap rocks as volatile pressures associated with the original diorite melt exceeded lithostatic pressures on the melt. Fragments in the breccia vary in size from 1/4 inch to approximately 10 feet on their long dimension. In general, there is very little diorite matrix in the breccia, which, as a result, has the appearance of randomly jumbled, welded blocks of rock. The limits of brecciation are difficult to define because of generally poor exposure. On the basis of surface exposures, brecciation occurs only between the center and north base lines and lines 24 W to 52 W (Figure 6). The age of brecciation is at least that of the D_2 deformation since fabric elements associated with that event are affected by brecciation. A more probable age is mid to late Cretaceous since quartz-monzonite of the Anvil Batholith gives potassium-argon ages of 90-95 m.y. and is cut by the diorites. Moderately large, angular blocks of banded, highly weathered, massive sulfides occur in the breccia near line 36 W between the center and north base lines. These sulfides represent the brecciated northeast extension of zone 3 and will be discussed in a later section.

Another breccia is exposed near the intersection of line 8 W and the North Fork of Rose Creek. The preponderance of fragments in this breccia are calc-silicate gneiss averaging less than 2 feet along their maximum dimensions. Hornblende diorite, again the matrix of the breccia, shows moderate amounts of sphalerite and galena mineralization. A representative analysis of the breccia indicates the following metal values: (not available)

A relatively minor, medium grained, equigranular, dark pink monzonite intrudes the breccia. This phase seems to follow joint surfaces in the existing breccia and appears to be later than the main phase of brecciation. It is unmineralized. Source of the base metals in the diorite is possibly an eastern extension of the Number 2 zone intruded by the diorite. The presence of the calc-silicate gneiss fragments in the biotite-muscovite schist unit remains unexplained. An irregular, subsurface intrusive diorite body centered on line 16 W between the central and south base lines may be the parent of the diorite causing brecciation.

Intrusion of smokey quartz-feldspar porphyry, minor muscovite granite and leucocratic, tourmaline-garnet monzonite dikes is the last recognizable intrusive event on the Faro grid. In the absence of definitive cross cutting relationships, intrusion of these granitic rocks is considered to be one event. Since the muscovite granite and monzonite dikes cut hornblende diorite dikes and the porphyry cuts a breccia most probably produced by diorite intrusion, these granitic rocks are considered to be younger than the diorite clan.

In summary, four intrusive rock sequences are recognized on the Faro grid. On the basis of cross cutting relationships, the amphibolites are the oldest recognizable intrusive unit since they are cut by the S_2 foliation (D_2 metamorphism is Ordovician according to Templeman-Kluit)? The next recognizable event is the intrusion of the Cretaceous Anvil Batholith. Hornblende diorites intrude the batholithic rocks and brecciate the Eocambrian metamorphic rocks near inferred centers of diorite intrusion. Late stage granitic and monzonitic dikes cut rocks of the diorite clan and breccia produced by it.

Deformational History:

Rocks on the Faro grid have the same geometry and deformational history as those in the pit. All of the structural features described in the pit, including its deformational history, apply to rocks on the grid.

The S_1 foliation is best developed in the biotite-muscovite phyllite unit. Most phyllite outcrops show well developed F_2 folds in S_1. In general, these folds are parallel to similar and have sub-equal limb heights. S_2, the active plane of movement, is axial planar to these folds which are developed on all scales. Commonly F_2 folds have limb heights of fractions of inches to several inches. In large outcrops, limb heights of 10 to greater than 100 feet are observed. These larger scale F_2 folds are not commonly seen because of prevailing small outcrop size. Thin to laminar compositional banding parallel to S_1 emphasizes F_2 folds in outcrop. Occasionally, S_1 seems to show a consistent attitude in outcrop suggesting either a uniformly dipping, undeformed, penetrative, regional metamorphic foliation or, more likely, a uniformly dipping portion of a large F_2 fold limb. Attitudes of such large planar S_1 surfaces strike 120°-150° and dip sub-vertically. Axes of F_2 folds trend 120°-150° with a cluster around 140° and plunge shallowly northwest or southeast parallel to the L_2 crenulation lineation. Figure 3 summarizes this geometry.

F_2 folds are not as well preserved in the calc-silicate gneiss and biotite-muscovite schist emphasizing the difference in mechanical behaviour of the different stratigraphic units. Since F_2 folds are better preserved in the gneiss than the schist, the latter appears to have behaved in a more ductile manner during D_2. The gneiss in turn showed more ductile behaviour than the phyllite. The general absence of F_2 folds in the massive sulfides exposed in the pit suggests they have the lowest ductility contrast with other units in the stratigraphic pile.

As in the pit, banding in the calc-silicate gneiss and biotite-muscovite schist parallels the main, penetrative S_2 foliation. Banding in the phyllite only parallels S_2 on limbs of F_2 folds further suggesting its high ductility contrast. In addition, the major stratigraphic unit contacts (or regional compositional banding) parallel S_2 giving rise to a regional "layer cake" stratigraphy. The inferred mechanical behaviour of the different units suggests that compositional banding on

all scales represents S_1 banding variably transposed into parallelism with S_2 by the D_2 deformation. Transposition in the schists was complete, in the gneisses nearly complete, and in the phyllites incomplete.

On the scale of the grid, the F_3 folds and L_3 lineation are the only recognizable D_3 structural features. S_3 is developed sporadically in some mesoscopic F_3 folds. L_3 is penetrative on the scale of the grid and can be recognized in nearly all outcrops. F_3 folds of varying scale occur in all rock types. Macroscopic F_3 folds are developed along the southern margin of the Anvil Batholith on the west grid. These folds are parallel, flexural slip folds overturned slightly to the northeast. Their axes trend [redacted]° and plunge [redacted]° to the [redacted]. Amplitudes of these structures vary from 100 to 800 feet with wavelengths of 1800 to 3200 feet (Figures 6 and 8). The close spatial association of these folds and the batholith suggests a genetic connection. Inspection of cross-section BB' (Figures 6 and 8) shows that the batholith cuts the F_3 folds making a genetic relationship suspect. It is possible these folds developed in response to ~~initial diapiric upwelling of the batholith which on its later stages of intrusion cut the folds.~~

D_4 features superimposed on the existing poly-deformational fabric include F_4 folds and the L_4 lineation. The L_4 lineation can be found in most outcrops in the gneiss and phyllite units. Because of its coarsely porphyroblastic nature, the muscovite-biotite schist does not preserve this linear feature. Two macroscopic assymetric, flexural slip, parallel, overturned F_4 folds, termed the ~~Faro anticline and syncline~~, have been defined on the grid. (Figures 6, 7, 8, 9, 10, 11, 12, 14, 15) These folds in the S_2 foliation give rise to the repetition of stratigraphic units seen on the grid (Figure 6). Their amplitudes are approximately [redacted] to [redacted] feet over wavelengths of approximately 6000 feet. Axes of these folds trend 110° to 130° and plunge to the [redacted] on the west grid at about [redacted]°. On the east grid, the axis of the Faro anticline becomes horizontal and the Faro syncline is cut out by the Anvil Batholith. Both folds are overturned to the north on the west grid (Figures 6, 7 and 8). Their sense of overturning and style is identical to that of the F_4 folds in the pit on the south limb of the anticline (Figures 2 and 4). For these reasons, the smaller scale F_4 folds in the pit are considered to be congruent and parasitic to the Faro anticline. The genetic relation (if any)

between these folds and the Cretaceous Anvil Batholith is unclear. Arguments similar to those waged for the F_3 folds and their relation to the batholith could be put forward here as well. In general, these arguments are not compelling since both the F_3 and F_4 fold generations show marked intrusive contacts with the batholith (Figures 6, 7, 8, 10, 11, 12, 14 and 16). In addition, the hornblende diorite body at the north end of the pit cuts the F_4 folds and is probably genetically related to the batholith. Therefore, the F_3 and F_4 folds and the deformational events which produced them are probably pre-Cretaceous in age.

D_5 deformational features are seldomly encountered on the Faro grid emphasizing the subsidiary role of this event. Warps in S_2 over the Faro orebodies have geometries similar to F_5 folds but additional work is needed to affirm the connection. Very occasional, mesoscopic F_5 folds are found in the grid rocks and the L_5 lineation is only seen in these instances.

The last recognizable deformational event on the Faro grid is a period of brittle faulting. Two main faults appear to bound the number three orebody on its northwest and southeast margins (Figure 6). The [redacted] is postulated on the northwest to account for large, apparent offsets in the sulfide mass. Movement along this fault is normal with the [redacted] side [redacted]. There is no surface expression of this fault as it occurs in an area of no outcrop. NORTH FORK ~~Big Indian~~'s fault bounds zone 3 on the southeast and is, in all likelihood, a ~~right lateral~~, [redacted], [redacted]. The normal component of its movement produces large, apparent offsets in the sulfide mass by downdropping the northwest block to form a graben over zone 3. The strike slip component of its movement appears to separate zones 2 and 3 (Figures 6, 16 and 17) which, prior to faulting, were probably part of the same sulfide mass. Big Indian's fault is well exposed along line 36 W between the center and north base lines as a mylonite zone 15 to 20 feet in width dipping to the northwest (Figure 6). It cuts an irregular, dike-like mass of smokey quartz feldspar porphyry in this area which is Cretaceous or younger in age. For this reason, faulting is considered the last deformational event in the area. Two minor, left lateral, transcurrent faults subparallel to the [redacted] and Big Indian's fault offset the contact between the gneiss and phyllite units on the west grid.

Metamorphism associated with each deformational event is identical to that outlined for these events in the pit. The S_1 and S_2 foliations are penetrative on the scale of the grid. D_1 metamorphism is, at least, biotite grade (lower greenschist facies) and probably higher, while D_2 metamorphism, assiciated with the main deformational event, is lower to middle amphibolite facies rank. The depositional, deformational and intrusive history of the Faro area is summarized in Figure 18.

Relationship of Sulfides to Stratigraphy and Structure:

All lead-zinc sulfide occurrences of note on the Faro grid are found in the [redacted] unit approximately 200-300 feet beneath the contact with the overlying calc-silicate gneiss. This interval is characterized by abundant graphitic schist units and is similar to the stratigraphic sequence above the Faro number one orebody as seen in the pit. These relationships provide a valid exploration guide for rocks in the immediate Faro area. Each known occurrence of sulfides in this area will be discussed in this section.

The [redacted] are situated on the [redacted] of the Faro [redacted] (Figures 6, 9, 10, 11, 12, 13, 14 and 15) in the favourable stratigraphic interval. Section CC' (Figure 9) shows the broad relations of structure in the pit to the Faro anticline. F_4 folds in zone 1 are seen to be [redacted] and [redacted] to the anticline (compare Figures 4, 8 and 9). Extensions of the favourable stratigraphic horizon would logically be expected on the north limb of the anticline. Mapping on this portion of the fold failed to reveal graphitic schist and/or quartzite units. Exploration drilling has confirmed the absence of significant sulfide mineralization in this area but occasional graphitic quartzites have been intersected (DDH 64-D4, Figure 13). These intersections occur 200-300 feet beneath the calc-silicate gneiss suggesting irregular continuations of the favourable horizon across the fold axis.

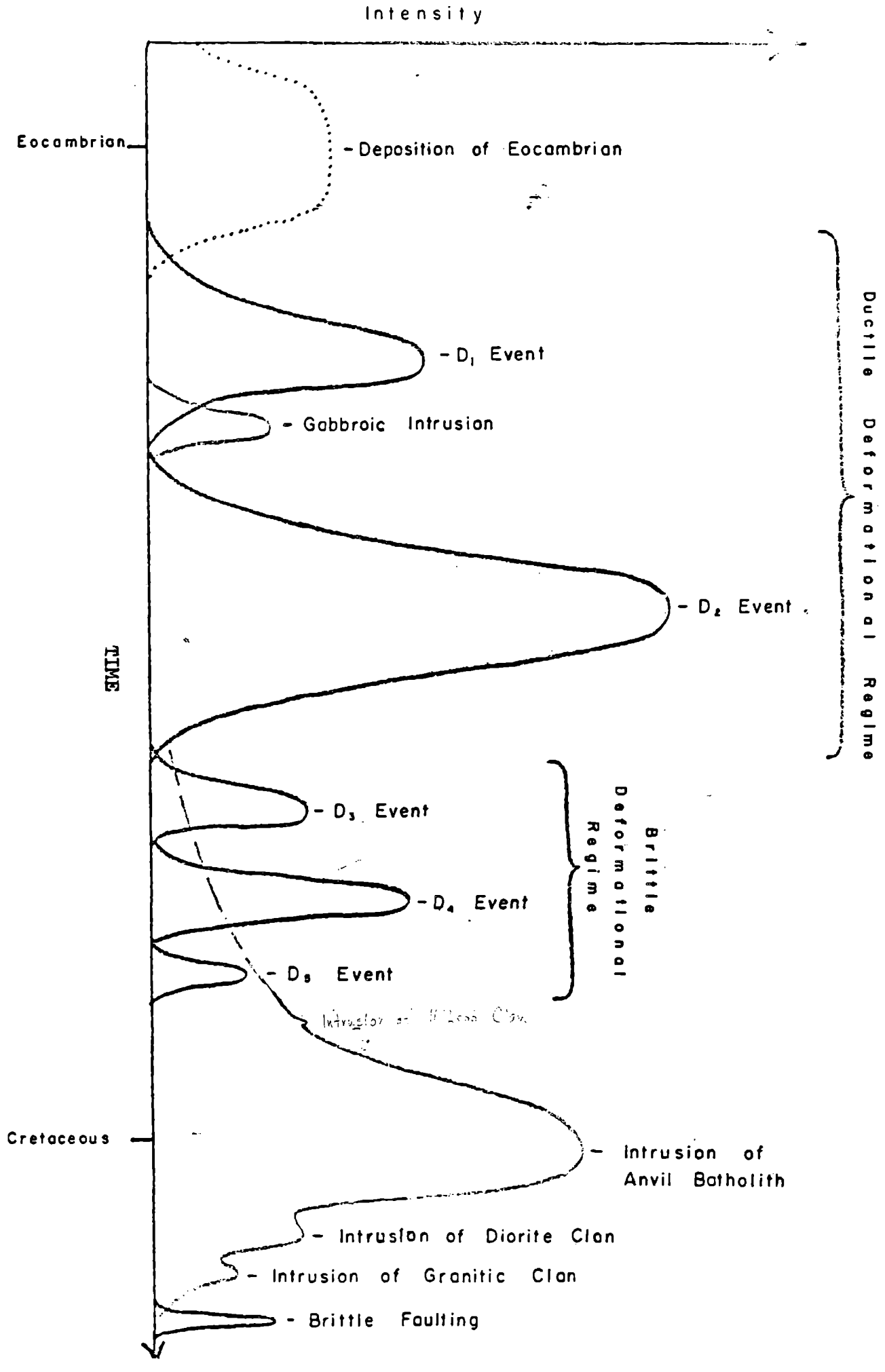

FIGURE 18: SEQUENCE OF GEOLOGIC EVENT, FARO AREA

Sulfide blocks in the breccia over zone 3 have already been described. Cross section FF' (Figure 12) shows that these blocks are the brecciated, up-dip extension of zone 3 sulfides on the south limb of the Faro anticline.

Banded massive and disseminated sulfides occur in graphitic schists at the top of DDH 71-210 (Figure 6). On the basis of banding conformity to S_2, the sulfide zone is thought to dip to the southwest in accordance with S_2 in nearby outcrops. Because of their stratigraphic separation from zones 2 and 3, these sulfides are considered to be a separate zone (Figures 13, 14 and 15). Alternatively, they may be an extension of zone 2 which is discordant to S_2 (Figure 15). If this were the case, DDH-71-217 should have intersected sulfides as well. Exploration drilling in the vicinity of this occurrence suggests the sulfides to be of limited extent. Additional definition drilling is proposed.

Sulfide mineralization was also encountered in FRH-2. No structural data could be obtained from the drill log since it was a rotary hole. Consequently, it is not known whether the sulfides encountered were brecciated or not (see Figure 6). Considering the depth of intersection and general structure of the areas, it is simplest to treat this intersection as another zone dipping to the southwest along the south limb of the Faro anticline (Figures 12, 13 and 15). It does not seem likely that sulfides in FRH-2 and DDH 71-210 are related since DDH 71-216, located between them (Figure 6), encountered no mineralization.

The possibility of zones 2 and 3 once being continuous across Big Indian's fault has already been mentioned. Structural relationships in this area are shown in Figures 16 and 17. The broad, open, anticlinal warp in Figure 17 is possibly related to the D_5 event since its axis trends about 60°. Development drilling in this area should clarify the question of sulfide continuity.

Brecciated, massive sulfides are found in the Faro Creek diversion ditch over zone 2 on line 24 W south of the south base line (Figure 6). These sulfide blocks are caught up in a heavily weathered and altered muscovite granite. Cross section JJ' (Figure 16) shows that these blocks were stoped into the granite body as it intruded zone 2 and were transported upward to their present position.

Finely crystalline galena and moderate amounts of marcasite and pyrite have been found in thin quartzites interbanded with graphitic schists southeast of the junction of the North Fork and main tote road. The quartzites and graphitic schists occur a few hundred feet beneath the contact with the calc-silicate gneiss in the biotite-muscovite schist and represent an extension of the favourable stratigraphic horizon enclosing zone 2. While no economic mineralization has been encountered in drilling to date, the occurrence emphasizes the association of mineralization, quartzites and graphitic schists beneath the calc-silicate gneiss.

Geological Investigations in Other Areas:

Several areas on the southern flank of the Anvil Arch have been investigated in reconnaissance fashion. These areas include portions of the Ed-Gal-Bill, Sun-Tie-Gal and Dy-Rich-Bob claim groups (Figure 1).

Unit contacts from the Faro grid can be traced into the Ed-Gal-Bill claims (Figure 1). The strong curvature of these contacts reflects the interaction of shallowly dipping stratigraphic units and topography. No fold structures affecting these contacts are mappable in this area. Rock units on this claim group lie on the south flank of the Faro anticline and dip fairly uniformly to the southwest. Features related to at least the D_1, D_2, D_3 and D_4 events are recognized. One of the most interesting geological features in this area is the presence of moderately thick bands of amphibolite in sharp contact with the biotite-muscovite phyllite. In all probability, the amphibolites are the metamorphosed equivalent of basaltic intrusions or flow rocks. They probably accumulated as an integral part of the stratigraphic sequence and are pre - D_2 in age since they are cut by S_2.

Mapping on selected portions of the Sun-Tie-Gal and Dy-Rich-Bob claim groups was undertaken to assess the structural and stratigraphic environment of the Vangorda, Champ and Firth sulfide deposits. The areas investigated are underlain by the biotite muscovite phyllite unit (Figure 1). The above-mentioned deposits all occur within this unit and are associated with graphitic horizons. Quartzites and muscovite-rich phyllites are reported to occur with the Vangorda deposit.

The basal portion of the phyllite unit appears to be more muscovite rich and less calcareous than the upper portion and the phyllite unit on the Faro grid. Preliminary whole rock analytical data do not support this contention.

Amphibolite units similar to those encountered on the Ed-Gal-Bill claims are interbanded with the phyllites. Fine grained, gray-green, thinly laminated calc-silicate units commonly envelope the amphibolites. Perhaps these units are metamorphosed tuffaceous horizons associated with basaltic submarine (?) flow rocks now re-crystallized to amphibolites.

Excellent examples of S_1 and F_2 folds are encountered routinely in these rocks. In general, the entire deformational picture for rocks on the Faro grid applies here. S_1 is seen to be transposed parallel to S_2 on the limbs of F_2 folds while remaining relatively undeformed in the hinge zones. In some cases, transposition along F_2 limbs has been severe enough to produce "rootless folds" i.e. detached hinge zones.

The L_3 lineation is probably present in this area, but it may not have the same attitude as seen on the Faro grid. Systematic mapping of the Faro fabric elements from the North Fork to Blind Creek is required to relate rock geometries in the two areas. F_4 folds can be mapped with a fair measure of certainty in the Vangorda area. An overturned anticline-syncline pair occurs on the Sun-Tie-Gal claims while the Vangorda anticline is the dominant F_4 structure on the Dy and Rich claims (Figure 1).

Review of Geological Relationships:

Three stratigraphic units have been defined in the Eocambrian sequence in the Anvil district. In ascending stratigraphic order, they are: a) biotite muscovite schist b) calc-silicate gneiss and c) biotite-muscovite phyllite. Five deformational events have

been superimpose l on this sequence before intrusion of the Anvil Batholith. The :wo earliest deformational events occurred at higher grades of regional metamorphism than the latter three. Rocks of the Anv .l district behaved in a ductile manner during the D_1 and D_2 ev :nts with the production of slip folds and transposition of stratigraphic contacts. The D_3, D_4 and D_5 events took plac : under conditions of brittle behaviour, characterized by the productic ı of crenulation lineations and flexural slip folds. Sulfide deposits associated with quartzites, muscovite schists and graphitic sc ıists occur in the biotite-muscovite schist and biotite-muscovit : phyllite; the Faro orebodies occur in the former, Vangorda , Swim, Champ and Firth in the latter.

Origin of Rock Units:

Metamorphic Rocks:

The general pelitic bulk composition of the major stratigraphic units leaves little doubt of their sedimentary origin. Known igneous rocks do not show the high SiO_2 and Al_2O_3 contents as well as the high K_2O/Na_2O ratios seen in analyses of the main stratigraphic units in the Anvil district.[1] Presence of graphitic schists and quartzites in the schist and phyllite units and marbles in the calc-silicate gneiss lend support to this argument since these interbanded units are most often developed in sedimentary environments. The most probable mode of accumulation of the entire Eocambrian section is quiet water deposition of pelitic debris in a euxinic marine basin. A marine origin is suspected because of the regional development of the units and their high calcium carbonate content. The schist and phyllite units may represent transgressive sedimentary facies, the calc-silicate gneiss a regressive sequence from a stable, miogeosynclinal shelf enrironment. Thus, the entire section may represent a sedimentary "off lap" cycle. Graphite in the schist and phyllite units strongly suggests accumulation under reduced conditions in a restricted basin. Source of the carbon may have been decaying algal matter from a proximal carbonate stable shelf area. Quartzites in the schist and phyllite units may be metamorphosed channel fills from the same shelf area. Amphibolites in the phyllites probably represent submarine flows from miogeosynclinal vent centers or island areas.

[1] Thirty whole rock analyses have been completed on rocks from the Anvil district. Accuracy problems preclude their inclusion in this report.

Sulfides:

A syngenetic model of sulfide accumulation is favoured. The intimate association of sulfides with metasedimentary rocks and their lack of immediate spatial assoction with intrusive or extrusive igneous rocks rocks suggests sulfide deposition is related to accumulation of the stratigraphic pile. Sulfides in, at least, the Faro number one orebody are stratabound in a quartzite unit. All other occurrences of mineralization in the district are directly associated with graphitic schists. Since quartzites and graphitic schists are almost undoubtedly of sedimentary parentage, the sulfides are considered syngenetic. Sulfur isotopic data shows similar isotopic fractionation between sulfur in the Faro orebodies and sulfur in Cambrian sea water sulfate suggesting sulfur, in at least the Faro deposits, was derived from sea water. At any rate, the observed fractionations in the Faro sulfides bear no resemblance to those in hydrothermal deposits. A sea water source for sulfur compliments a syngenetic depositional model. The reduced depositional environment inferred for the graphitic portions of the stratigraphic section fits with the need to reduce sea water sulfate to the sulfide radical.

Regional geologic studies militate against sulfides being related to the Anvil Batholith on several grounds. There is no convincing spatial association of batholithic rocks with any sulfide deposit in the district. In fact, hornblende diorites, presumably a late stage intrusive phase of the batholith, cut Faro number one implying the sulfides are older than, at least, the diorites. Batholithic rocks have been shown to cut fold structures affecting Faro zone 1 further demonstrating the older age of the sulfides (Figure 8). Mapping in the district by Templeman-Kluit has shown that the fabric produced, by what is here termed the D_2 event, is not developed in rocks younger than Ordovician age. Since this event affects all the known sulfide deposits in the district, they must be at least Ordovician. Potassium-argon methods date the Anvil Batholith as mid-Cretaceous.

For these reasons, sulfide deposits in the Anvil district are thought to be syngenetic and Precambrian in age. Because of the large concentrations of base metals as discreet deposits, rapid accumulation of sulfides is indicated. Rapid accumulation implies either high rates of base metal input into the depositional environment or conditions of sea water saturation with respect to lead and zinc. Lead-zinc rich volcanic exhalations or erosion of pre-existing sulfide deposits could provide base metal sources in either manner to combine with sulfur reduced from sea water sulfate.

Implications of Sulfide Origin and Deformational History to Exploration:

If a syngenetic origin for the sulfide deposits of the Anvil district is accepted, original bedding, S_o, in sandstone and carbonaceous shale units in the schist and phyllite protoliths appears to be the primary structural control for localization of sulfide deposition. Thus, it is important to trace the original sandstones (now quartzites) and carbonaceous shales (now graphitic schists) through the deformed metamorphic pile in the Anvil district on a regional scale as well as a local one. Locally, graphitic schists, quartzites and muscovite schists have been traced within a restricted stratigraphic interval of the schist unit on the Faro grid.

Similar intervals in the phyllite unit remain to be defined and traced thru the district along with those in the schist unit. In this connection, understanding the early deformational history of the Anvil belt becomes important in defining at what scale folding may duplicate the stratigraphic section. F_3 and F_4 folding occurs on known scales and can be used to trace stratigraphic horizons. The effects of the D_1 and D_2 events are obscured by these later events. Consequently, less is known about them even though they are responsible for much of the rock fabric in the area. The following paragraphs summarize deformation associated with these early periods of folding and their relevance to exploration.

Possible, post - D_2, pre - D_3 topologies of S_o can be determined through consideration of several deformational models based on limiting structural conditions. These conditions are tabulated below:

1) ~~S_o was originally horizontal.~~

2) ~~S_1 is a metamorphic foliation found during D_1 in which, at least, biotite was stable.~~

3) Strong compositional banding (laminar to 1 foot thick) is coincident with S_1.

4) F_2 folds have subequal limb heights.

5) S_2 transposes S_1 into parallelism with itself on F_2 fold limbs and is the active, D_2, deformational element.

6) S_1 is subvertical in F_2 fold hinges.

7) The main stratigraphic units in the Eocambrian sequence are concordant to S_2 over moderately large areas of the district.

8) F_3 and F_4 folds flex S_2 into open to close flexural slip folds.

9) The Anvil Arch is a mid-Cretaceous dome in S_2 formed by intrusion of the Anvil Batholith.

Unfolding of the Anvil Arch and the F_3 and F_4 folds results in subhorizontal S_2 and stratigraphic unit attitudes. Assuming that only the D_3, D_4, and D_5 events occur between D_2 and formation of the arch, S_2 must have been subhorizontal after the D_2 event. This condition must then be the end product of any analysis of the D_1 and D_2 events.

Beginning with initial deposition of rock units in the Anvil belt, several deformational paths can be taken by originally horizontal bedding, S_o, to arrive at this condition. With the onset of D_1 metamorphism, S_1 can either develop parallel or at an angle to horizontal bedding, S_o. These two alternatives cover all possible attitudes of S_1 development but variable behaviour of S_1 during D_1 deformation is possible. Three illustrative cases will be treated: 1) S_1 develops parallel to S_o 2) S_1 develops at an angle to S_o with minimal transposition of S_o and 3) S_1 develops at an angle to S_o with considerable transposition of S_o. These cases are diagrammed in Figure 19. In each case, S_2 must have a subhorizontal attitude after the D_2 event and resultant rock geometry must satisfy all the limiting conditions in the above list.

Case 1:

S_1 develops parallel to S_o as a bedding plane foliation of, at least, biotite grade during D_1.[o] This is the most specialized case for S_1 development. If S_2 is constrained to a subhorizontal attitude after the D_2 event, it must be subparallel to S_1 and S_o. Clearly this violates conditions 4, 5 and 6 since no F_2 folds would ever be produced.

Templeman-Kluit considers S_1 a bedding plane foliation as in this model, but treats S_2 as though it dipped at a moderate angle to the southwest during D_2.[2] In this way, S_2 folds S_1 and S_o into F_2 folds with unequal limb heights. His model is at odds with the probable subhorizontal attitude of S_2 prior to doming of the Anvil Arch. It appears as though he used the post-Cretaceous attitude of S_2 on the south flank of the arch and related D_2 deformation to that attitude. Even if S_2 did dip gently to the southwest, F_2 folds in S_2 and S_o produced by active slip along S_2 would have unequal limb heights contravening condition 4. Templeman-Kluit's model is included in Figure 19 for comparative purposes.

Case 2:

S_1 develops at an angle to S_o producing F_1[1] folds with minimal transposition of S_o into parallelism with the axial planar S_1 foliation. Recrystallization of S_o results in the production of laminar banding parallel to S_1 by "metamorphic differentiation." S_2 creates mesoscopic F_2 folds on the limbs of larger F_1 folds (i.e. in S_o) and in the S_1 foliation. This model meets all the required conditions and is attractive in that it requires essentially no bedding transposition, allowing regional conformity of stratigraphic unit contacts to S_2 and original bedding.

[1] F_2 folds are slip folds in S_o to which S_1 is probably axial planar. They are not seen in rocks of the Anvil district.

This model is not without problems. If "metamorphic differentiation" did occur during D_1 recrystallization, in all likelihood, bedding transposition would have occurred under these ductile conditions as well. In addition, it is doubtful that "metamorphic differentiation" could produce compositional banding at the scales observed under the grades of metamorphism experienced during D_1. This model would also permit preservation of large numbers of F_1 folds which are not seen in rocks of the Anvil district.

Case 3:

S_1 develops at an angle to S_0 producing F_1 folds with large amounts of bedding transposition parallel to the axial planar S_1 foliation. F_2 slip folds produced during D_2, refold the F_1 generation folds obliterating their hinges and transposing S_1 and S_0 parallel to S_2. This model satisfies all the limiting conditions and fits the observed mechanical behaviour of rocks in the Anvil area. It is proposed as a working model of regional D_1 and D_2 deformation subject to revision with additional work.

If the deformational model proposed as Case 3 is correct, exploration implications become apparent. Macroscopic F_2 nappe structures could exist on all scales in the Anvil metamorphic belt. If the stratigraphic unit shaded in Case 3, Figure 19, is considered to be a favourable, quartz-rich graphitic schist horizon, knowledge of its topology increases exploration potential in areas of nappe development.

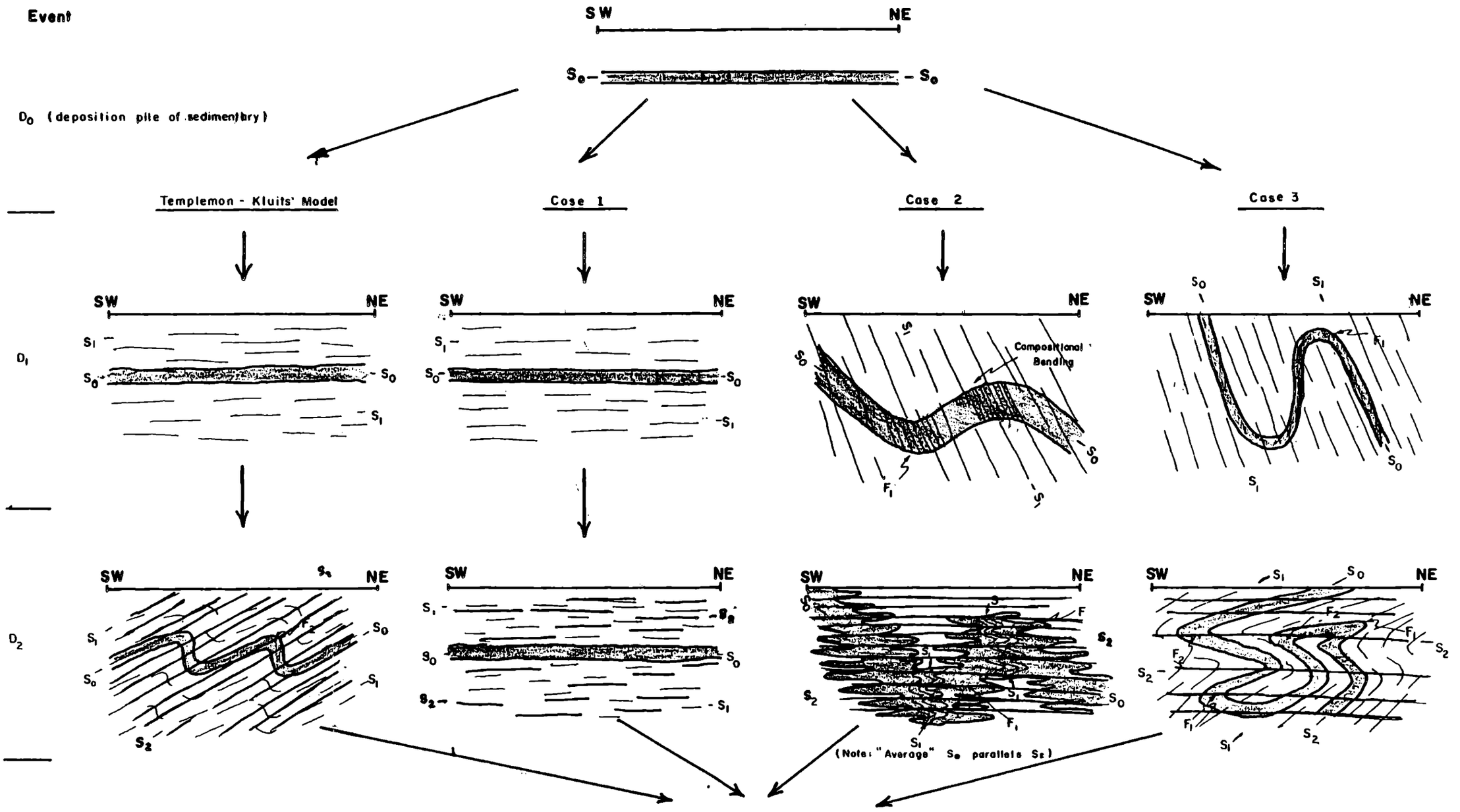

FIGURE 19: D_1 & D_2 Deformational Models

MINE ELEVATIONS

Mine elevations are 109.24 higher than m.s.l. due to survey defferance at original station. TRI 18.
See surveyors for details

RST
Nov. 182